analytical chemistry

Article

pubs.acs.org/ac

Exonuclease III-Aided Autocatalytic DNA Biosensing Platform for Immobilization-Free and Ultrasensitive Electrochemical Detection of Nucleic Acid and Protein

Shufeng Liu,[†,‡] Ying Lin,[‡] Li Wang,[‡] Tao Liu,[‡] Chuanbin Cheng,[‡] Wenji Wei,[‡] and Bo Tang*[,†]

[†]College of Chemistry, Chemical Engineering and Materials Science, Collaborative Innovation Center of Functionalized Probes for Chemical Imaging, Key Laboratory of Molecular and Nano Probes, Ministry of Education, Shandong Normal University, Jinan, Shandong 250014, P. R. China

[‡]College of Chemistry and Molecular Engineering, Qingdao University of Science and Technology, Qingdao, Shandong 266042, P. R. China

Supporting Information

ABSTRACT: Homogenous electrochemical biosensor has attracted substantial attention owing to its simplicity, rapid response, and improved recognition efficiency compared with heterogeneous biosensor, but the relatively low detection sensitivity and the limited detection analytes prohibit its potential applications. To address these issues, herein, a simple, rapid, isothermal, and ultrasensitive homogeneous electrochemical DNA biosensing platform for target DNA and protein detection has been developed on the basis of an exonuclease III (Exo III)-aided autocatalytic target recycling strategy. A ferrocene-labeled hairpin probe (HP1) is ingeniously designed, which contains a protruding DNA fragment at 3′-termini as the recognition unit for target DNA. Also, the DNA fragment that could be used as secondary target analogue was introduced, but it was caged in the stem region of HP1. In the presence of target DNA, its recognition with the protruding fragment of HP1 triggered the Exo III cleavage process, accompanied with the target recycling and autonomous generation of secondary target analogues. This accordingly resulted into the autonomous accumulation of ferrocene-labeled mononucleotide, inducing a distinct increase in the electrochemical signal owing to its elevated diffusivity toward indium tin oxide (ITO) electrode surface. The autocatalytic biosensing system was further extended for protein detection by advising an aptamer hairpin switch with the use of thrombin as a model analyte. The current developed autocatalytic and homogeneous strategy provided an ultrasensitive electrochemical detection of DNA and thrombin down to the 0.1 and 5 pM level, respectively, with a high selectivity. It should be further used as a general autocatalytic and homogeneous strategy toward the detection of a wide spectrum of analytes and may be associated with more analytical techniques. Thus, it holds great potential for the development of ultrasensitive biosensing platform for the applications in bioanalysis, disease diagnostics, and clinical biomedicine.

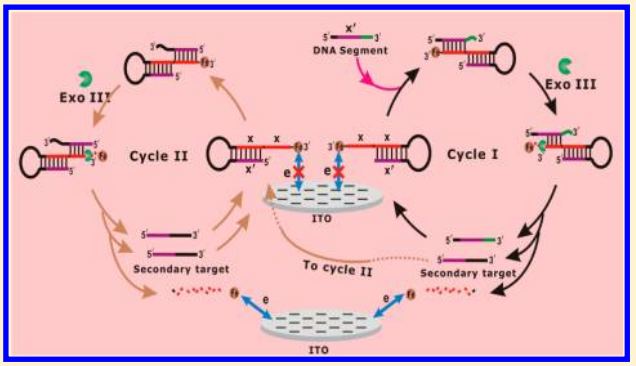

During the past decades, more and more biomarkers, for example, nucleic acids, protein, and enzymes, have been largely disclosed to be directly correlated with the occurrence and development of some severe diseases such as cancers.[1−4] It has been generally recognized that, in the early stage of disease, the concentrations of relevant biomarkers are usually on a relatively low level. Thus, the development of biosensor capable of amplified detection of target analyte is highly desirable to satisfy the requirement of profiling the trace amounts of biomarker and then serve in the clinical diagnosis and medical treatment of diseases.[5−8] Until now, various signal amplification strategies have been pursued to explore the extreme detection capability toward target analytes.[9,10] Especially, the development of autocatalytic biosensor has drawn more and more concerns owing to its striking improvement for the detection sensitivity toward target analytes.[11,12] Similar with the conventional target recycling strategy, it is usually operated with the involvement of various nucleases, including endonuclease, polymerase, exonuclease, etc., for the signal amplification. The unique characteristics are the autonomous generation of new target analogues accompanied with the typical target recycling process, which corresponds to indirectly amplifying the amounts of target analytes. Thus, it holds a great promise to substitute polymerase chain reaction (PCR) due to its easy operation and isothermal reaction. In this respect, the autonomous replication−scission−displacement process based on nicking endonuclease and polymerase has been widely

Received: January 29, 2014
Accepted: March 24, 2014
Published: March 24, 2014

   dx.doi.org/10.1021/ac500426b | *Anal. Chem.* 2014, 86, 4008−4015

Table 1. Sequences of Oligonucleotides Used in the Experiments[a]

name	sequence (from 5′ to 3′)
HP1	AGACTAGACCGGAACGACGGTCTAGTCT *GTCTAGTCT*-Ferrocene
HP2	ACCAGTCATCGGAACGACGATGACTGGT *GTCTAGTCT*-Ferrocene
HP3-a	**GGTTGGTGTGGTTGGAATAGACTAGACTATTCCAACCACACCTGGTG**
HP3-b	**GGTTGGTGTGGTTGGAATAGACTAGACTATTCCAACCACTGGTG**
HP3-c	**GGTTGGTGTGGTTGGAATAGACTAGACTATTCCAACTGGTG**
target DNA	ATTAGACTAGACTATTCC
1MT-DNA	ATTAGTCTAGACTATTCC
2MT-DNA	ATTAGTTTAGACTATTCC
NC-DNA	CGGTACGCCGGTAGAGTG

[a]The underlined letters in HP represent the complementary base sequences. The italicized letters in HP3 and target DNA are the same base sequences and are complementary with the italicized letters in HP1 and HP2. The boldface letters in HP3 indicate the aptamer sequence for thrombin.

employed for the autocatalytic amplified detection toward different biomolecules.[13−18] More recently, the quadratic enzymatic amplification strategy has also been proposed for miRNA and cytokines detection, respectively, based on the combination of nicking endonuclease, exonuclease, and polymerase.[19,20] However, the employment of multiple nucleases affects the assay cost and also may increase the risk of false-positive signal output toward target detection. Furthermore, the autocatalytic recycling amplification system based on the use of sole exonuclease, endonuclease, or DNAzyme has also been developed for the fabrication of ultrasensitive biosensors,[21−23] yet it is confronted with the requirement of relatively complex probe or procedure design. In this context, the development of a simple, rapid, isothermal, and autocatalytic amplification system is highly desirable for the applications in biomolecule diagnostics.

The fluorescence-based optical detection method is the most widely used means for the fabrication of the amplified biosensing system owing to its ease to operate in the homogeneous solution,[24] while it is not so easily amenable to the development of cost-effective and low-power hand-held readout devices. By comparison, the electrochemical method can provide significant advantages, such as simple and portable instrumentation, rapid response, low cost, and high sensitivity.[25−27] However, almost all the electrochemical biosensors are based on the heterogeneous assay that often involve the immobilization of recognition element on the electrode. The proper immobilization strategy is thus demanded, and the immobilization step is usually laborious and time-consuming. Also, as the recognition to analyte occurs on the interface between the solution and electrode, the configurational freedom of the immobilized recognition unit is often restricted owing to the steric hindrance effect of the electrode surface, accompanied by the relatively low binding efficiency and rate of recognition unit toward its substrate. Thus, the development of faster and easier-to-use immobilization-free electrochemical strategies is highly desirable. Very recently, Xuan et al. proposed a homogeneous electrochemical strategy for the detection of target DNA.[28] It opens a promising direction for the development of homogeneous electrochemical biosensors.[29−34] However, the detection sensitivity of these previous endeavors in homogeneous electrochemical DNA biosensors is still far from that of the superior heterogeneous electrochemical biosensors. Also, the developed homogeneous electrochemical strategy mainly focuses on the trial for target DNA detection. Therefore, upgrading the detection sensitivity of homogeneous electrochemical biosensor to make it rival or even exceed that of the heterogeneous electrochemical biosensor and extending the detection analytes beyond nucleic acid remain two major and urgent challenges in the development of a homogeneous electrochemical biosensor.

Herein, a simple and novel exonuclease III (Exo III)-aided autocatalytic target recycling strategy was proposed and integrated with the homogeneous electrochemical method for the achievement of ultrasensitive assay of DNA and protein. A 3′-ferrocene labeled hairpin probe (HP1) is ingeniously designed, which consists of a protruding single-stranded DNA fragment at the 3′-termini as the recognition unit for target DNA. The 3′-strand for the stem region of HP1 possesses the same base sequence with the protruding DNA fragment, but it is hybridized by the complementary base sequence. By this design, the DNA fragment that can serve as a secondary target analogue is introduced but is caged in the stem region of HP1. In the presence of target DNA, its recognition with the protruding fragment of HP1 triggers the Exo III cleavage process, accompanied with the target recycling and autonomous generation of secondary target analogue. This accordingly results in the autonomous accumulation of ferrocene-labeled mononucleotide. On the basis of the diffusivity difference between the generated ferrocene-labeled mononucleotide and the ferrocene-labeled HP1 toward indium tin oxide (ITO) electrode surface, an autocatalytic and homogeneous electrochemical DNA biosensing platform for ultrasensitive and immobilization-free detection of target DNA was developed. It was further extended for protein detection with the recommendation of an aptamer hairpin switch strategy with the use of thrombin as a model analyte. The current developed autocatalytic strategy should be easily extended for the detection toward a wide spectrum of analytes including nucleic acid, protein, nuclease activity, and biological small molecules. Furthermore, the developed autocatalytic DNA biosensing strategy could be also easily associated with some other analytical techniques, for example, fluorescence, colorimetry, etc. Thus, it shows a huge potential for the development of an ultrasensitive biosensing platform for biomolecular detection in bioanalysis and clinical biomedicine.

EXPERIMENTAL SECTION

Reagents. The HPLC-purified oligonucleotide sequences were purchased from Sangon Biotech. Co., Ltd. (Shanghai, China) and listed in Table 1. Exonuclease III was purchased from New England Biolabs Ltd. (Ipswich, MA, USA) and used without further purification. Human thrombin was supplied by Dingguo Biotech Co., Ltd. (Beijing, China). Lysozyme was

dx.doi.org/10.1021/ac500426b | Anal. Chem. 2014, 86, 4008−4015

Scheme 1. Schematic Illustration of Exo III-Assisted Autocatalytic Biosensing Platform for the Immobilization-Free Detection of Target DNA

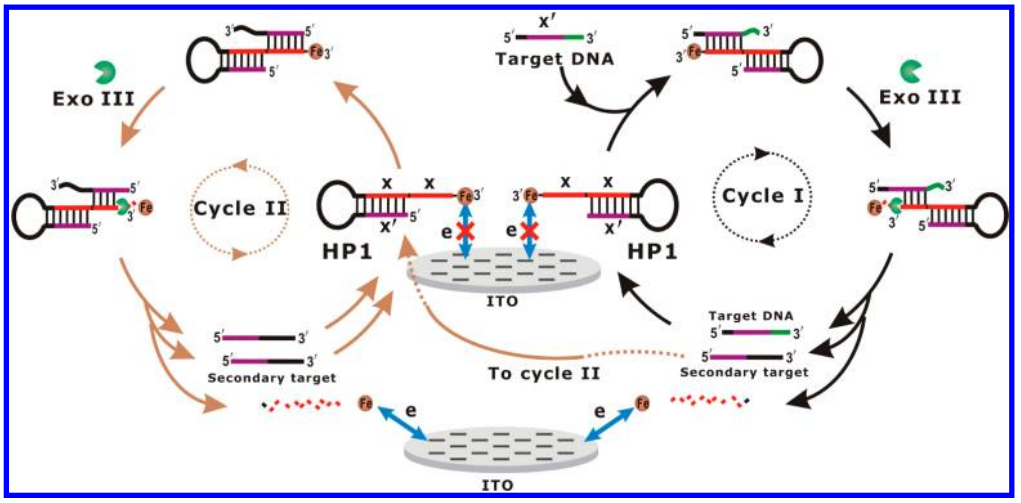

bought from Tiangen Biotech Co, Ltd. (Beijing, China). Bovine serum albumin (BSA) and human IgG were purchased from Sangon Biotech. Co., Ltd. (Shanghai, China). All other chemicals were of analytical grade and used as received.

Exo III-Aided Autocatalytic DNA Recycling. 50 μL of 10 mM Tris-HCl buffer (pH 7.6, 10 mM $MgCl_2$, 10 mM KCl, 50 mM NaCl) containing 2 μM ferrocene-labeled HP1 or HP2, 100 units of Exo III, and varying concentrations of the target DNA was incubated at 37 °C for 30 min and then used for the electrochemical experiments.

Protein Detection. The detailed procedure for the detection of model analyte of protein thrombin was as follows. First, the aptamer hairpin probe (HP3) was mixed with different concentrations of thrombin at 37 °C for 30 min to form the aptamer probe−target complex. Second, the ferrocene-labeled HP1 and Exo III were added to the solution and incubated at 37 °C for 30 min. The final concentrations of HP1, HP3, and Exo III in the last solution were 2 μM, 100 nM, and 2 unit/μL, respectively. The same reaction mixtures without thrombin were used as negative controls.

Electrochemical Characterization. Electrochemical measurements were conducted on a CHI 832B electrochemical analyzer (CH Instruments Inc., Shanghai, China) with a conventional three-electrode system comprising an ITO working electrode, a platinum wire auxiliary electrode, and a Ag/AgCl reference electrode. Before each electrochemical measurement, the ITO electrode was sequentially sonicated in an Alconox solution (8 g of Alconox/L of water), propan-2-ol, acetone, and water, each for 10 min. Then, the electrode was immersed into 1 mM NaOH solution for 5 h at room temperature and sonicated in water for 10 min. After these procedures, a negatively charged working electrode surface was obtained. The differential pulse voltammogram (DPV) was recorded in the above-mentioned 50 μL incubation buffer containing reaction mixtures with the potential window from 0.05 to 0.75 V.

RESULTS AND DISCUSSION

Design Principle of the Sensor. The new autocatalytic and immobilization-free electrochemical strategy for ultrasensitive detection of nucleic acid was demonstrated in Scheme 1. A hairpin DNA probe (HP1) was ingeniously designed, which consisted of two sequential domains **X** at 3′-termini, the loop region and the domain **X**′ at 5′-termini. The base sequence in domain **X**′ was complementary with that of the domain **X**. In order to achieve the hybridization of domain **X**′ with the adjacent but not the distal domain **X**, two extra base-pairs were introduced in the stem region of HP1 to increase the hybridization stability. Thus, the HP1 shows a stabilized stem-loop structure with the protruding fragment (domain **X**) at the 3′-end, which can be recognized by target DNA or target response-released DNA segment. The 3′-end of HP1 was labeled with a ferrocene tag, and it could resist the digestion by Exo III since the 3′-end was in a single-strand configuration. The Exo III has been well recognized to specifically cleave duplex DNA from blunt or recessed 3′ termini.[35−38] Therefore, the ferrocene-labeled HP1 would exhibit only a negligible electrochemical response on the sensing electrode owing to the electrostatic repellence from the negative ITO electrode. When the HP1 was challenged with target DNA, the recognition of target DNA with the dangling base sequence of domain **X** at the 3′-end of HP1 by a template enhanced hybridization process led the HP1 to have a blunt 3′-terminus.[37] Exo III then could catalyze the stepwise removal of mononucleotides from this terminus, resulting in the release of the target DNA and ferrocene-labeled mononucleotide. The released target DNA was free to bind to another 3′-protruding terminus of HP1 to trigger a new cleavage process, and thus, the autonomous cyclic formation of the free ferrocene-labeled mononucleotide was activated, which constituted of the Cycle I in Scheme 1. The ferrocene-labeled mononucleotide cleaved off by Exo III possesses much higher diffusivity toward negatively charged ITO electrode owing to the reduced electrostatic repulsion than that of ferrocene-labeled HP1, leading to a distinct increase in the electrochemical signal.[28,29] Furthermore, accompanied with each cleavage process in Cycle I, a new DNA fragment including the base sequence in the loop region and domain **X**′ of HP1 was also released, which could be used as a secondary target analogue to further hybridize with the protruding fragment **X** at the 3′ end of HP1. Following its recognition with the ferrocene-labeled HP1 and the cleavage process by the Exo III, the secondary target trigger could be again recycled or produced for a successive cleavage process, resulting in the continual generation of the ferrocene-labeled mononucleotide for amplified electrochemical response. This constituted the

dx.doi.org/10.1021/ac500426b | Anal. Chem. 2014, 86, 4008−4015

Cycle II in Scheme 1. On the basis of the autonomous cleavage in Cycles I and II, the target DNA trigger can be exponentially produced. Therefore, the current autocatalytic target recycling strategy by a simple Exo III-aided cleavage is hopeful for offering an ultrahigh sensitivity for the assay of nucleic acid. Furthermore, the autocatalytic and immobilization-free electrochemical sensing system was also extended for protein detection by the use of an aptamer probe switch as well as the use of thrombin as a model analyte. The corresponding content for protein detection will be discussed later in this work.

Exo III-Aided Autocatalytic DNA Biosensing Platform. To verify the feasibility of designed immobilization-free electrochemical amplified strategy for DNA detection, differential pulse voltammograms (DPV) obtained upon analyzing the DNA in the presence of Exo III and those obtained in a series of control experiments are depicted in Figure 1. As

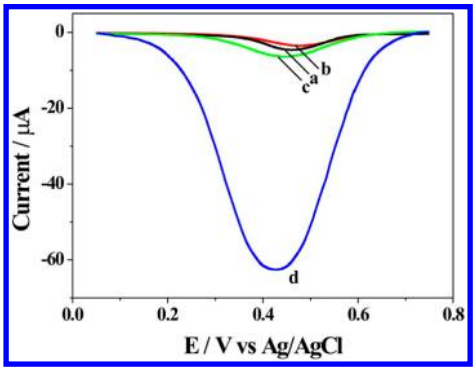

Figure 1. DPV responses of 50 μL of Tris-HCl buffer (pH 7.6) containing 2 μM HP1 after 30 min incubation, with (a) no target DNA, no Exo III, (b) 0.1 nM target DNA, no Exo III, (c) 2 unit/μL Exo III, no target DNA, and (d) 0.1 nM target DNA, 2 unit/μL Exo III.

shown in Figure 1d, a readily detectable DPV peak at around 0.43 V could be observed in the presence of target DNA and Exo III. This peak could be attributed to the electrochemical oxidation of the released ferrocene-labeled mononucleotide. However, in the absence of Exo III and target DNA, the signal of ferrocene was almost negligible (Figure 1a). The mere hybridization of ferrocene-labeled HP1 with target DNA would increase the electrostatic repellence from the negative electrode surface, resulting in the more weak electrochemical response (Figure 1b). Furthermore, a slightly increased electrochemical signal could be obtained in the presence of only Exo III (Figure 1c), which might be explained by the residual cleavage activity of Exo III toward the HP1 probe.[39,40] It should be also noted that the electrochemical response was only comparable with that in the presence of only Exo III when the non-complementary target DNA was used for control (data no shown), demonstrating the feasibility of the currently designed autocatalytic electrochemical strategy for target DNA detection.

Optimization of Experimental Conditions. In this assay, the initial amount of ferrocene-labeled HP1 plays an important role in the performance of the sensor. The HP1 probe concentrations were studied to probe the electrochemical performance toward the detection of 0.1 nM target DNA (Figure 2A). It could be found that the HP1 concentration of 2 μM could achieve the best signal-to-background ratio. The higher concentration of HP1 could result in a relatively high

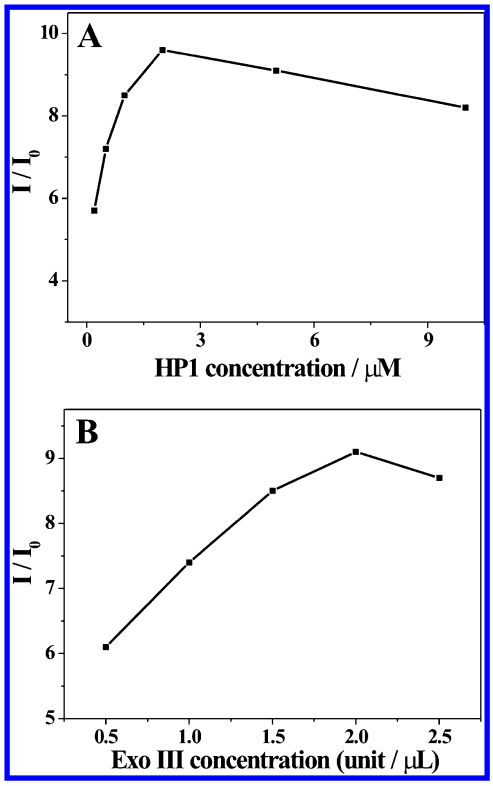

Figure 2. The optimization of HP1 probe concentration (A) and Exo III concentration (B). The I and I_0 are the electrochemical responses of the sensing system in the presence and absence of 0.1 nM target DNA, respectively.

background signal, which restricted the sensing performance for target DNA detection. The amount of employed Exo III was also optimized on the basis of the electrochemical response toward the detection of 0.1 nM target DNA (Figure 2B). It could be seen that the 2 unit/μL of Exo III could provide the best electrochemical response. The decreased electrochemical response at a higher amount of Exo III can be ascribed to the cleavage activity of Exo III toward HP1, resulting in a relatively high background signal. The time response of the fabricated autocatalytic sensing system toward the detection of 0.1 nM target DNA was also conducted (Figure 4D). It could be seen that the electrochemical signal increased continuously with the incubation time and almost reached the saturation value at a short incubation time of about 30 min. The signal saturation at 30 min suggested that the ferrocene-labeled mononucleotide was almost released from the HP1 for the electrochemical response.

Detection Performance of the Assay. Under the optimized experimental conditions, the detection performance of fabricated autocatalytic sensing system was investigated by using target DNA with different concentrations. As shown in Figure 3A, the DPV peak current increased with the concentration of target DNA ranging from 0 to 0.1 nM, indicating that the release of ferrocene-labeled mononucleotide was highly dependent on the concentration of target DNA. This also confirmed the working principle that the target DNA was hybridized with the HP1 to trigger the Exo III digestion. Figure 3B showed a good linear correlation of the DPV peak current of ferrocene to the logarithm of the concentrations of target DNA ranging from 0.1 pM to 0.1 nM with a correlation coefficient of 0.9941. The directly measured detection limit

dx.doi.org/10.1021/ac500426b | Anal. Chem. 2014, 86, 4008−4015

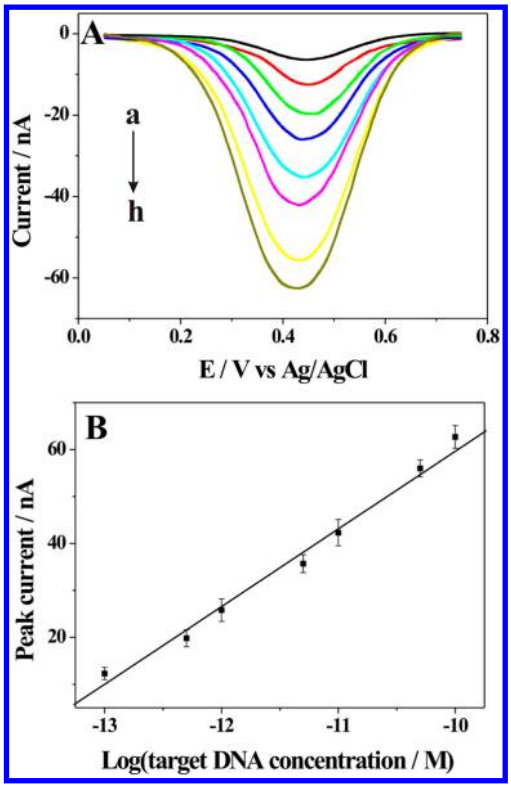

Figure 3. (A) Differential pulse voltammograms corresponding to the analysis of different concentrations of target DNA. The concentrations of target DNA for the curves (a) to (h) are: (a) 0 pM, (b) 0.1 pM, (c) 0.5 pM, (d) 1 pM, (e) 5 pM, (f) 10 pM, (g) 50 pM, and (h) 0.1 nM. (B) The linear plots of DPV peak currents vs the logarithm of target DNA concentrations. The error bars represented the standard deviation of three repetitive measurements.

toward target DNA was as low as 0.1 pM, providing superior or comparable detection sensitivity compared with those reported electrochemical methods (Table S1 in the Supporting Information). The results demonstrated that this signal amplification method was efficient for ultrasensitive electrochemical detection of DNA hybridization.

To further prove the signal amplification effect of currently developed autocatalytic target recycling strategy, another ferrocene-labeled hairpin probe (HP2) was also designed as a substitute of HP1 for comparison, which contained also the dangling fragment (**X**) complementary with the partial sequence of target DNA. The difference for HP2 with the advised HP1 lies in that the base sequences in the stem region of HP1 (the hybrids of **X**–**X**′) are substituted by arbitrarily complementary base sequences. That is, the recognition of target DNA with HP2 could also trigger the cleavage process of Exo III toward HP2 and resulted in the release of the target DNA and ferrocene-labeled mononucleotide, but no new target analogues could be generated. Thus, only target DNA but no secondary target DNA analogues could be recycled to trigger the successive cleavage process (Figure 4A). It was denoted as a typical Exo III-aided target recycling strategy. This typical target recycling strategy was also explored for the detection toward different concentrations of target DNA (Figure 4B). The electrochemical response increased linearly with the logarithm of target DNA concentrations ranging from 10 pM to 1 nM (Figure 4C). It could only achieve a detection limit of about 10 pM for target DNA. Also, it should be noted that the electrochemical response to target DNA by the autocatalytic recycling strategy at the same concentration was significantly higher than that by the typical recycling strategy. Furthermore, it could be seen from Figure 4D that the developed autocatalytic recycling strategy could achieve a more rapid electrochemical response before reaching equilibrium compared with that of a typical recycling strategy, indicating again that the autocatalytic recycling process indeed occurred.

Selectivity of the Fabricated DNA Biosensor. The specificity of the developed autocatalytic DNA sensing system was further investigated by using four kinds of DNA sequences, including complementary target DNA, single-base mismatched DNA (1MT-DNA), two-base mismatched DNA (2MT-DNA), and noncomplementary DNA (NC-DNA) at the same concentration of 0.1 nM. As shown in Figure 5, the DPV peak currents for 1MT-DNA and 2MT-DNA were about 34.1% and 17.9% of that for perfect target at the same concentration, respectively. The NC-DNA showed almost the same response with the blank solution. Thus, this method exhibited a good performance to discriminate perfect complementary target and the base mismatched targets and held great potential for single nucleotide polymorphism analysis.

Analytical Performance of Protein Detection. The developed autocatalytic DNA biosensing platform was further extended for protein detection. As a proof-of-concept, human thrombin was chosen as the model analyte of interest, which played an important role in the thrombosis, hemostasis, and many coagulation-related reactions.[41,42] The levels of thrombin concentration have been well-known to be closely associated with some diseases, including thromboembolic disease and Alzheimer's disease.[43] Conventionally, the protein detection is executed by using two aptamers in order to form a sandwich structure.[44] Herein, a target-responsive aptamer hairpin switch toward thrombin was designed, which could circumvent the limitations of sandwich assays.[45,46] As shown in Figure 6A, the aptamer hairpin probe (HP3) contained three sections: thrombin aptamer (red), target DNA sequence (T-DNA, violet) and extend-DNA sequence (E-DNA, green). E-DNA was designed to be complementary to a part of the aptamer, in order to stabilize the hairpin-shape form of the HP3 in the absence of thrombin. The design of the complementary domain of HP3 was also to prevent the hybridization of T-DNA sequence to HP1 probe in the absence of target protein. The binding of aptamer to thrombin unzipped the double-stranded aptamer/E-DNA of the HP3. HP3 was energetically more stable when aptamer binding to the thrombin formed the aptamer/thrombin complex, causing the HP3 to adopt the open form. The exposed single stranded T-DNA could easily hybridize with the dangling fragment of HP1 to trigger the successive cleavage process by Exo III toward HP1. The T-DNA was thus considered to play the same role with the above-referred target DNA and trigger the autocatalytic DNA recycling process and lead to the release of the ferrocence-labeled mononucleotide for the amplified electrochemical signal toward thrombin detection. Additionally, the high binding activity of aptamer/protein could effectively remain with the developed autocatalytic strategy owing to no modification or immobilization of aptamer probe.

In order to make sure that the T-DNA hybridized with the HP1 probe to trigger the successive Exo III-aided autocatalytic cleavage process only in the presence of the target protein, the E-DNA sequence was first optimized by using the HP3 with three different stem lengths. As shown in Figure 6B, the HP3

dx.doi.org/10.1021/ac500426b | *Anal. Chem.* 2014, 86, 4008–4015

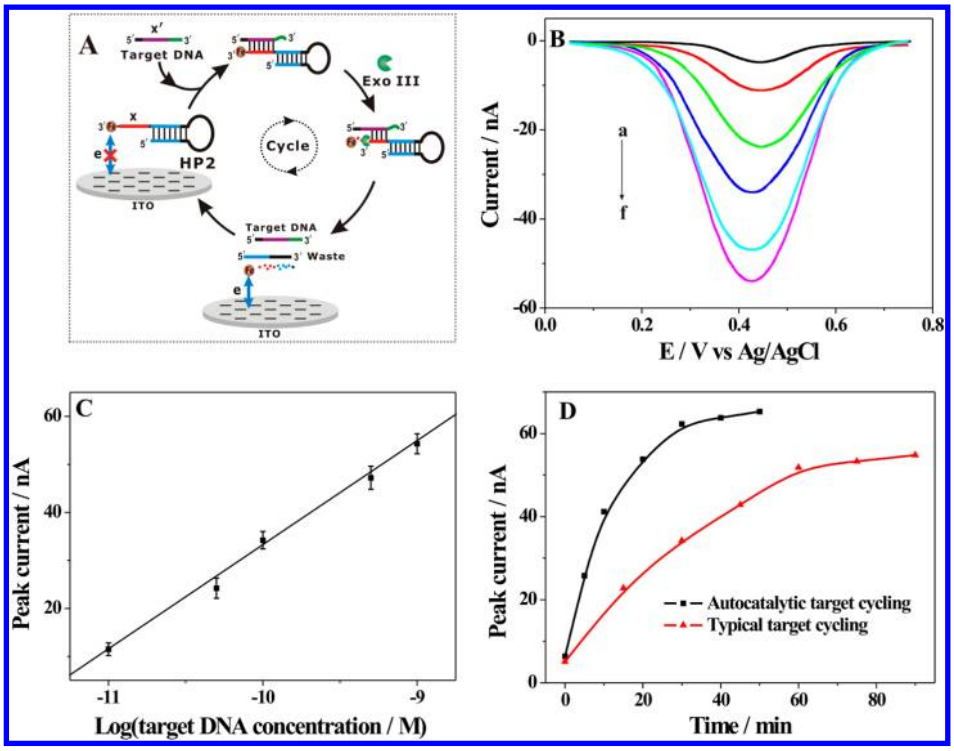

Figure 4. (A) Schematic illustration of the Exo III-aided typical target recycling strategy. (B) DPV responses of the sensing system recorded after an incubation time of 30 min toward the analysis of different concentrations of target DNA: (a) 0 pM, (b) 10 pM, (c) 50 pM, (d) 100 pM, (e) 500 pM, and (f) 1 nM. (C) The linear plot of DPV peak currents vs the logarithm of target DNA concentrations. The error bars represented the standard deviation of three repetitive measurements. (D) The time responses of the fabricated autocatalytic sensing system and the Exo III-aided typical target recycling system toward the detection of 0.1 nM target DNA.

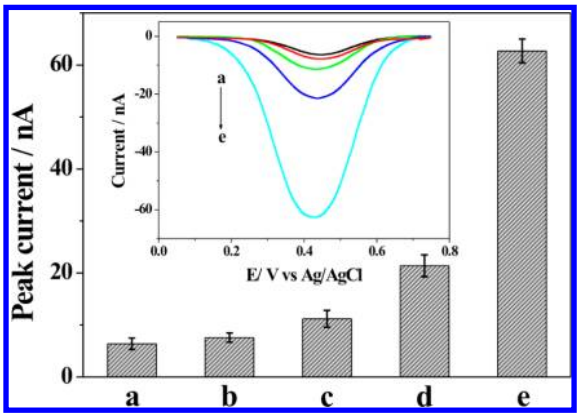

Figure 5. The bar chart of the DPV responses toward the blank (a) and the four various DNA sequences including (b) NC-DNA, (c) 2MT-DNA, (d) 1MT-DNA, and (e) complementary target DNA. The concentrations of various DNA sequences were all 0.1 nM. The error bars represented the standard deviation of three repetitive measurements. The inset showed the corresponding DPV responses.

containing the stem length of 8 base-pairs could give the best analytical results compared with that of the HP3 containing 5 and 11 base-pairs in the stem region. For this optimized HP3, the E-DNA of HP3 perfectly matched thrombin aptamer with 8 base-pairs. When the stem length was too long, the binding efficiency between aptamer and thrombin were not good enough for the opening of the hairpin probe, and when the matched base-pairs between thrombin aptamer and E-DNA were only 5, the hairpin probe was unstable. Thus, we chose HP3 with the stem length of 8 base-pairs for the following experiments. To further confirm the ability of the described autocatalytic strategy to sensitively detect target protein, a series of different concentrations of thrombin ranging from 0 to 1 nM were measured (Figure 6C). The electrochemical intensity was observed to increase with the concentrations of thrombin, indicating that more ferrocene-labeled mononucleotides were released for the accumulation of the electrochemical signal. Again, the electrochemical response in the absence of thrombin was relatively low because the T-DNA sequence could only be liberated and hybridized with the dangling fragment of HP1 in the presence of target protein. The plot of the DPV peak currents of ferrocene with the logarithm of the concentrations of thrombin showed a good linear relationship in the range from 5 pM to 1 nM with a correlation coefficient of 0.9927 (Figure 6D). The directly measured detection limit could be obtained as low as 5 pM, indicating superior or comparable detection sensitivity compared with those reported electrochemical methods (Table S2 in the Supporting Information). This high sensitivity could be ascribed to the large signal amplification effect of the developed autocatalytic sensing strategy. The thrombin detection was also conducted by the typical target recycling strategy with the replacement of HP1 by HP2 (Figure S1Ain the Supporting Information). A low detection limit of about 200 pM could only be obtained (Figure S1B in the Supporting Information), indicating again the robust amplification ability of the developed autocatalytic sensing system for protein detection, but in the thrombin detection, the formed aptamer/thrombin complex may impose some restrictions on the accessibility of the exposed T-DNA sequence in HP3 toward HP1 or HP2 and even the cleavage activity of Exo III toward HP1 or HP2. This might contribute to the difference in detection performance toward thrombin and target DNA.

dx.doi.org/10.1021/ac500426b | Anal. Chem. 2014, 86, 4008−4015

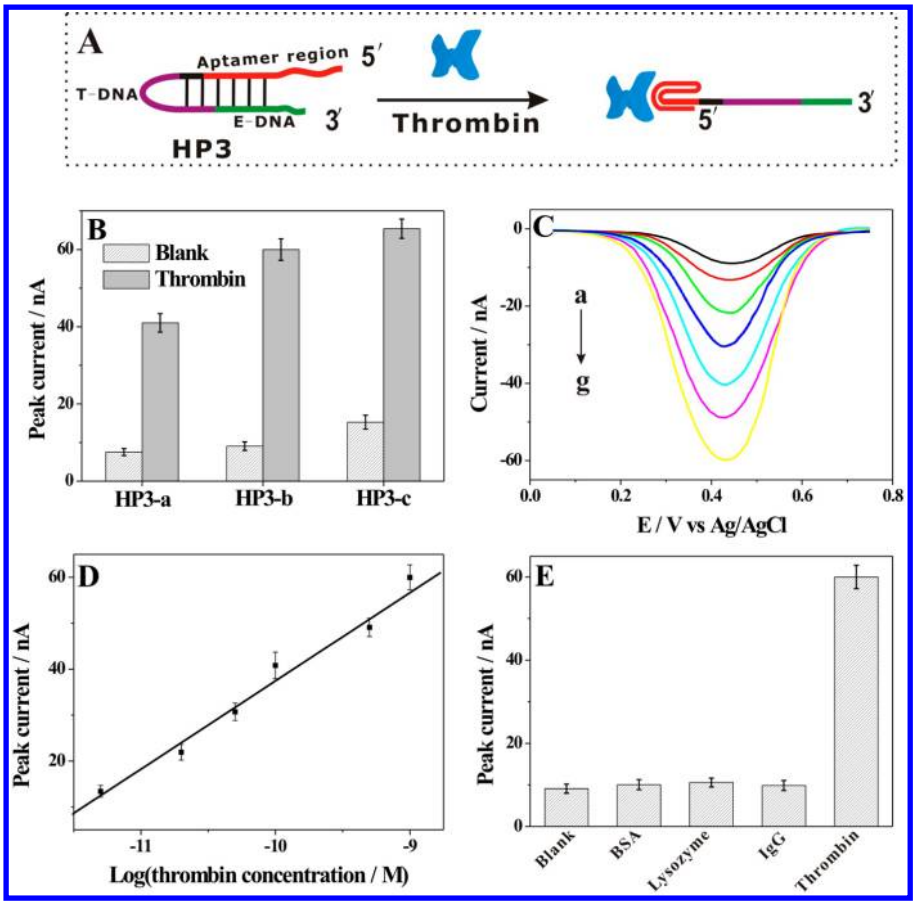

Figure 6. (A) Aptamer hairpin switch for thrombin recognition. (B) Sequence optimization of hairpin aptamer probe (HP3). The numbers of matched base-pairs for thrombin aptamer region of HP3: HP3-a, 11; HP3-b, 8; HP3-c, 5. The concentrations of the thrombin sample were 1 nM. (C) DPV responses corresponding to the analysis of different concentrations of thrombin. The concentrations of thrombin for the curves (a) to (g) are: (a) 0 pM, (b) 5 pM, (c) 20 pM, (d) 50 pM, (e) 100 pM, (f) 500 pM, and (g) 1 nM. (D) The linear plot of DPV peak currents vs the logarithm of thrombin concentrations. (E) The specificity of the assay for human thrombin and other proteins including BSA, lysozyme, and IgG. The concentrations of the employed proteins were all 1 nM. The error bar was calculated from three independent experiments.

The selectivity of the described herein method for thrombin detection was further investigated by examining the electrochemical responses of system toward BSA, IgG, and lysozyme. The system only showed a remarkable electrochemical response in the presence of thrombin. Nevertheless, in the presence of three other kinds of nonspecific proteins, the electrochemical response was negligible (Figure 6E), demonstrating that the electrochemical signal was specifically triggered by the aptamer/target binding for parallel samples. The above experiments revealed that the proposed sensing system could offer a high sensitivity and be excellent for protein assay.

CONCLUSIONS

A simple, rapid, isothermal, ultrasensitive, and homogeneous electrochemical DNA biosensing platform for target DNA and protein detection was developed on the basis of an ingeniously designed Exo III-aided autocatalytic target recycling strategy. The detection limit toward target DNA and thrombin was achieved to be as low as 0.1 and 5 pM, respectively, which could rival or even exceed that of the reported excellent heterogeneous electrochemical biosensors. Moreover, it exhibited the distinct advantages of simplicity in probe design and biosensor fabrication and rapidness in a recognition and detection process. Furthermore, the developed autocatalytic and homogeneous biosensing strategy should be fairly easy to extend for the detection of a wide spectrum of analytes including nucleic acid, protein, nuclease activity, and biological small molecules and be associated with some other analytical techniques. Thus, it opens a promising avenue to develop the autocatalytic and immobilization-free electrochemical biosensing of analytes for the applications in bioanalysis and clinical biomedicine.

ASSOCIATED CONTENT

Supporting Information

Additional information including thrombin detection by the typical target recycling strategy and the comparison of detection performance for current homogeneous electrochemical biosensor with those reported electrochemical methods. This information is available free of charge via the Internet at http://pubs.acs.org/.

AUTHOR INFORMATION

Corresponding Author

*Tel/Fax: +86 531 86180017. E-mail: tangb@sdnu.edu.cn.

Notes

The authors declare no competing financial interest.

■ ACKNOWLEDGMENTS

This work was supported by 973 Program (2013CB933800), National Natural Science Foundation of China (21227005, 21390411, 91313302, 21035003, and 21005043), Program for Changjiang Scholars and Innovative Research Team in University, the Basic Research Program of Qingdao (No. 13-1-4-214-jch), and the Science Foundation of China Postdoctor (No. 2012M511537).

■ REFERENCES

(1) Sawyers, C. L. *Nature* **2008**, *452*, 548−552.
(2) Wood, S. L.; Knowles, M. A.; Thompson, D.; Selby, P. J.; Banks, R. E. *Nat. Rev. Urol.* **2013**, *10*, 206−218.
(3) Kulasingam, V.; Diamandis, E. P. *Nat. Clin. Pract. Oncol.* **2008**, *5*, 588−599.
(4) Rusling, J. F.; Kumar, C. V.; Gutkind, J. S.; Patel, V. *Analyst* **2010**, *135*, 2496−2511.
(5) Turner, A. P. F. *Chem. Soc. Rev.* **2013**, *42*, 3184−3196.
(6) Song, S.; Qin, Y.; He, Y.; Huang, Q.; Fan, C.; Chen, H. Y. *Chem. Soc. Rev.* **2010**, *39*, 4234−4243.
(7) Lubin, A. A.; Plaxco, K. W. *Acc. Chem. Res.* **2010**, *43*, 496−505.
(8) Sefah, K.; Phillips, J. A.; Xiong, X.; Meng, L.; Simaeys, D. V.; Chen, H.; Martin, J.; Tan, W. *Analyst* **2009**, *134*, 1765−1775.
(9) Lei, J.; Ju, H. *Chem. Soc. Rev.* **2012**, *41*, 2122−2134.
(10) Wang, F.; Elbaz, J.; Orbach, R.; Magen, N.; Willner, I. *J. Am. Chem. Soc.* **2011**, *133*, 17149−17151.
(11) Weizmann, Y.; Cheglakov, Z.; Willner, I. *J. Am. Chem. Soc.* **2008**, *130*, 17224−17225.
(12) Wang, F.; Elbaz, J.; Willner, I. *J. Am. Chem. Soc.* **2012**, *134*, 5504−5507.
(13) Weizmann, Y.; Beissenhirtz, M. K.; Cheglakov, Z.; Nowarski, R.; Kotler, M.; Willner, I. *Angew. Chem., Int. Ed.* **2006**, *45*, 7384−7388.
(14) Zhang, C. Y.; Wang, G. L. *Anal. Chem.* **2012**, *84*, 7037−7042.
(15) Wang, F.; Freage, L.; Orbach, R.; Willner, I. *Anal. Chem.* **2013**, *85*, 8196−8203.
(16) Jia, H.; Li, Z.; Liu, C.; Cheng, Y. *Angew. Chem., Int. Ed.* **2010**, *49*, 5498−5501.
(17) Zeng, Y. P.; Hu, J.; Long, Y.; Zhang, C. Y. *Anal. Chem.* **2013**, *85*, 6143−6150.
(18) Zhang, Y.; Hu, J.; Zhang, C. Y. *Anal. Chem.* **2012**, *84*, 9544−9549.
(19) Duan, R.; Zuo, X.; Wang, S.; Quan, X.; Chen, D.; Chen, Z.; Jiang, L.; Fan, C.; Xia, F. *J. Am. Chem. Soc.* **2013**, *135*, 4604−4607.
(20) Zhou, W.; Gong, X.; Xiang, Y.; Yuan, R.; Chai, Y. *Anal. Chem.* **2014**, *86*, 953−958.
(21) Bi, S.; Li, L.; Cui, Y. *Chem. Commun.* **2012**, *48*, 1018−1020.
(22) Liu, S.; Zhang, C.; Ming, J.; Wang, C.; Liu, T.; Li, F. *Chem. Commun.* **2013**, *49*, 7947−7949.
(23) Wang, F.; Elbaz, J.; Teller, C.; Willner, I. *Angew. Chem., Int. Ed.* **2011**, *50*, 295−299.
(24) Zhang, H.; Li, F.; Dever, B.; Li, X. F.; Le, X. C. *Chem. Rev.* **2013**, *113*, 2812−2841.
(25) Ronkainen, N. J.; Halsall, H. B.; Heineman, W. R. *Chem. Soc. Rev.* **2010**, *39*, 1747−1763.
(26) Lubin, A. A.; Hunt, B. V. S.; White, R. J.; Plaxco, K. W. *Anal. Chem.* **2009**, *81*, 2150−2158.
(27) Xiao, Y.; Lou, X. H.; Uzawa, T.; Plakos, K. J. I.; Plaxco, K. W.; Soh, H. T. *J. Am. Chem. Soc.* **2009**, *131*, 15311−15316.
(28) Xuan, F.; Luo, X.; Hsing, I. M. *Anal. Chem.* **2012**, *84*, 5216−5220.
(29) Luo, X.; Lee, T. M. H.; Hsing, I. M. *Anal. Chem.* **2008**, *80*, 7341−7346.
(30) Miranda-Castro, R.; Marchal, D.; Limoges, B.; Mavré, F. *Chem. Commun.* **2012**, *48*, 8772−8774.
(31) Wu, J.; Huang, C.; Cheng, G.; Zhang, F.; He, P.; Fang, Y. *Electrochem. Commun.* **2009**, *11*, 177−180.
(32) Xuan, F.; Luo, X.; Hsing, I. M. *Anal. Chem.* **2013**, *85*, 4586−4593.
(33) Liu, S.; Wang, Y.; Zhang, C.; Lin, Y.; Li, F. *Chem. Commun.* **2013**, *49*, 2335−2337.
(34) Zhang, D. W.; Nie, J.; Zhang, F. T.; Xu, L.; Zhou, Y. L.; Zhang, X. X. *Anal. Chem.* **2013**, *85*, 9378−9382.
(35) Lee, H. J.; Li, Y.; Wark, A. W.; Corn, R. M. *Anal. Chem.* **2005**, *77*, 5096−5100.
(36) Zuo, X.; Xia, F.; Xiao, Y.; Plaxco, K. W. *J. Am. Chem. Soc.* **2010**, *132*, 1816−1818.
(37) Zhao, C.; Wu, L.; Ren, J.; Qu, X. *Chem. Commun.* **2011**, *47*, 5461−5463.
(38) Liu, X.; Aizen, R.; Freeman, R.; Yehezkeli, O.; Willner, I. *ACS Nano* **2012**, *6*, 3553−3563.
(39) Yang, Z.; Sismour, A. M.; Benner, S. A. *Nucleic Acids Res.* **2007**, *35*, 3118−3127.
(40) Xu, Q.; Cao, A.; Zhang, L.; Zhang, C. Y. *Anal. Chem.* **2012**, *84*, 10845−10851.
(41) Holland, C. A.; Henry, A. T.; Whinna, H. C.; Church, F. C. *FEBS Lett.* **2000**, *484*, 87−91.
(42) Gurm, H. S.; Bhatt, D. L. *Am. Heart J.* **2005**, *149*, S43−S53.
(43) Serruys, P. W.; Vranckx, P.; Allikmets, K. *Int. J. Clin. Pract.* **2006**, *60*, 344−350.
(44) Tennico, Y. H.; Hutanu, D.; Koesdjojo, M. T.; Bartel, C. M.; Remcho, V. T. *Anal. Chem.* **2010**, *82*, 5591−5597.
(45) Xue, L.; Zhou, X.; Xing, D. *Anal. Chem.* **2012**, *84*, 3507−3513.
(46) Li, J.; Fu, H. E.; Wu, L. J.; Zheng, A. X.; Chen, G. N.; Yang, H. H. *Anal. Chem.* **2012**, *84*, 5309−5315.